Synthesis of continuous silicon carbide fibre

Part 6 *Pyrolysis process of cured polycarbosilane fibre and structure of SiC fibre*

YOSHIO HASEGAWA
The Research Institute for Special Inorganic Materials, Asahi-mura, Kashima-gun, Ibaraki-ken 311-14, Japan

Polycarbosilanes which were synthesized by three methods were melt-spun and cured by heating at low temperatures in air. The curing mechanism and the structure of these cured fibres were studied and the relationship between the structure and the pyrolysis process is discussed. The structure of the cured fibre is represented by means of five structural elements and the rate of oxidation of the methyl group. The pyrolysis process of the cured fibre is discussed in five stages, and the effect of oxygen introduced into polycarbosilane fibre by curing on the pyrolysis process is clarified. The structure of the fibre obtained during the pyrolysis process strongly depends on the molecular weight of polycarbosilane.

1. Introduction

Polycarbosilanes (PC), which are the precursors of SiC fibre, have been synthesized by three methods and the molecular structures have been reported. Furthermore, the pyrolysis process of PC and the structure of the pyrolysis product were discussed [1]. In each PC, the silicon atoms forming the PC skeleton were represented by means of three simple elements: silicon bonded with four carbon atoms (SiC_4), silicon bonded with one hydrogen atom and three carbon atoms (SiC_3H), and silicon bonded with x carbon atoms and $(4 - x)$ silicon atoms (SiC_xSi_{4-x}, $x = 1, 2$ or 3) [1, 2]. The pyrolysis process of PC was divided into six temperature ranges [1]. In the first stage, evaporation of low molecular weight components in PC occurs, in the second the molecular weight of PC increases, in the third the side chains of PC decompose, in the fourth the products are amorphous in structure, in the fifth β-SiC is crystallized with an apparent crystalline size of 2 to 3 nm, and in the sixth crystal growth of β-SiC occurs.

In the present work, on the basis of the previous results [1, 2], the pyrolysis process of cured PC fibre and the structure of the pyrolysis product were discussed using PCs synthesized by three methods. It is important to investigate the effect of curing on the properties of SiC fibre. Curing is an important process in the industrial production of SiC fibre. In the curing process, PC fibre is heated at low temperature, so oxygen is introduced into the fibre. This oxygen should have an influence on the pyrolysis process of PC and the properties of the SiC fibre obtained. Part of the relationship between the oxygen content in PC fibre and the properties of SiC fibre has been reported [3]. In this report, the relationship is described in detail.

2. Experimental details

2.1. Synthesis and curing of polycarbosilane fibre

PC-TMS, PC-470 and PC-B (PC-B3.2 and PC-B5.5) were synthesized by three different methods [1]. The

molecular structure of each PC represented by three elements and the number average of molecular weight ($\bar{M}_n$) are shown in Table I [2].

These PCs were melt-spun in the same manner as in the previous report [4]. The PC fibres obtained were heat-treated at low temperatures in air and cured under the conditions shown in Table II. The weight gains after curing were measured.

2.2. Characterization of cured polycarbosilane

The structure of cured PC was analysed by infrared spectroscopy, thermal analysis (TG-DTA) in air and in nitrogen flow, chemical analysis and measurement of gas evolution during pyrolysis. These measurements were made by conventional means [1]. To determine the structure of cured PC from the infrared spectra, the KBr disc contained 0.668 mg of cured PC.

### 2.3. Characterization of the pyrolysis of cured polycarbosilane fibre

Characterization of the pyrolysis process of cured PC fibre was carried out by TG-TDA in a nitrogen flow, and, for the fibre pyrolysed at 400 to 1450° C in vacuum, by chemical analysis and measurements of infrared spectra, X-ray diffraction patterns and densities [1, 4]. In addition, the structure of the fibres obtained at 1200 and 1400° C was observed by transmission electron microscopy (TEM), using a JEOL JEM-2000CX electron microscope at 200 kV. The specimen for examination by TEM was prepared by picking up finely powdered fibre on a micromesh screen.

3. Results and discussion

3.1. Characterization of cured polycarbosilanes

In a previous paper [1], the pyrolysis process of PC was divided into six stages and the conversion of PC into SiC was discussed. In the method synthesizing SiC fibre in which PC is melt-spun, cured and then

Figure 1 TG-DTA curves of polycarbosilanes in air.
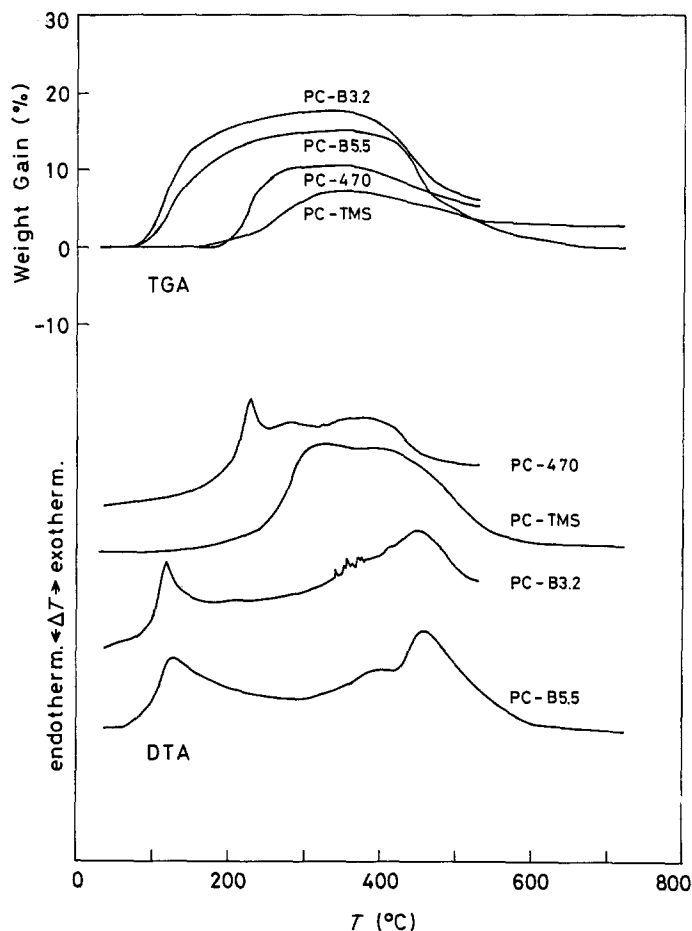
heat-treated at high temperature, the influence of curing, i.e. oxidation of PC, on the pyrolysis process of PC is important. Consequently, the structural change of PC induced by curing and the mechanism were discussed first.

As shown in Table II, the curing conditions and the weight gain after curing to become infusible in a subsequent process is characteristic of the synthesis method of PC. Weight gain by curing increases in the order PC-TMS < PC-470 < PC-B5.5 < PC-B3.2. The TG-DTA curve of each PC is shown in Fig. 1. The temperatures of exothermic peaks in the lower temperature region of DTA curves in PC-B3.2 and PC-B5.5 are lower than that of PC-470, in agreement with the temperature for weight gain to begin. The oxygen contents in cured PC fibres determined by chemical analysis and shown in Table III, are consistent with the prediction based on TG-DTA curves.

In the structural change of PC by curing, it has become apparent that the Si–H bond is oxidized and Si–OH, Si–O–Si and C=O bonds are formed [3, 4]. To

determine the change quantitatively, infrared difference spectra were synthesized by a point-by-point comparison of the two spectra before and after curing. These spectra are shown in Fig. 2. The absorbance of the infrared spectra after curing was corrected by multiplying by $W/(W - \Delta W)$ from Table II. As shown in Fig. 2, the absorbances of all the characteristic peaks of each PC were decreased by curing: 2950, 2880 and $2850\,cm^{-1}$ (C–H stretching), $2100\,cm^{-1}$ (Si–H stretching), $1400\,cm^{-1}$ (CH$_3$ deformation), $1350\,cm^{-1}$ (CH$_2$ deformation), $1250\,cm^{-1}$ (Si–CH$_3$ deformation, $1020\,cm^{-1}$ (CH$_2$ deformation in Si–CH$_2$–Si), $880\,cm^{-1}$ (Si–H deformation) and $820\,cm^{-1}$ (Si–CH$_3$ rocking and Si–C stretching) [1, 5]. On the other hand, the peaks at $3650\,cm^{-1}$ (free O–H stretching), 3600 to $3200\,cm^{-1}$ (O–H stretching), $1720\,cm^{-1}$ (C=O stretching), $1260\,cm^{-1}$ (Si–CH$_3$ deformation) and $1080\,cm^{-1}$ (Si–O stretching) appeared. From these results, for example, thermal oxidation of PC proceeds by the following mechanism
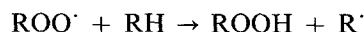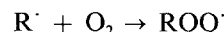
$$RH \rightarrow R^{\cdot} + H^{\cdot}$$

$$R^{\cdot} + O_2 \rightarrow ROO^{\cdot}$$

$$ROO^{\cdot} + RH \rightarrow ROOH + R^{\cdot}$$

TABLE I Fractions of SiC$_4$, SiC$_3$H and SiC$_x$Si$_{4-x}$ in polycarbosilanes, number average molecular weights ($\bar{M}_n$), and M_0^*

PC	SiC$_4$	SiC$_3$H	SiC$_x$Si$_{4-x}$	$\bar{M}_n$	M_0
PC-TMS	0.82	0.18	0	770	66.1
PC-470	0.53	0.47	0	1740	60.5
PC-B3.2	0.40	0.16	0.44	1740	56.9
PC-B5.5	0.44	0.15	0.41	1310	54.2

*Average molecular weight of a silicon atom calculated assuming that the average number of methyl groups bonded with a silicon atom are 1.61, 1.22, 1.42 and 1.23 for PC-TMS, PC-470, PC-B3.2 and PC-B5.5, respectively [2].

TABLE II Curing conditions of polycarbosilane fibres

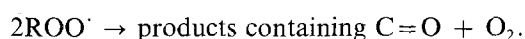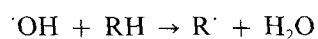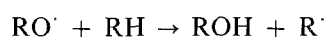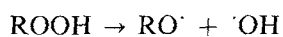| PC	Heating rate ($^{\circ}$C h^{-1})	Curing temp. ($^{\circ}$C)	Curing time (h)	Weight gain ($\Delta W/W$)
PC-TMS	10	200	1.0	0.0228
PC-470	33	190	0.5	0.0763
PC-B3.2	15	110	0.5	0.1684
PC-B5.5	15	110	0.5	0.1349
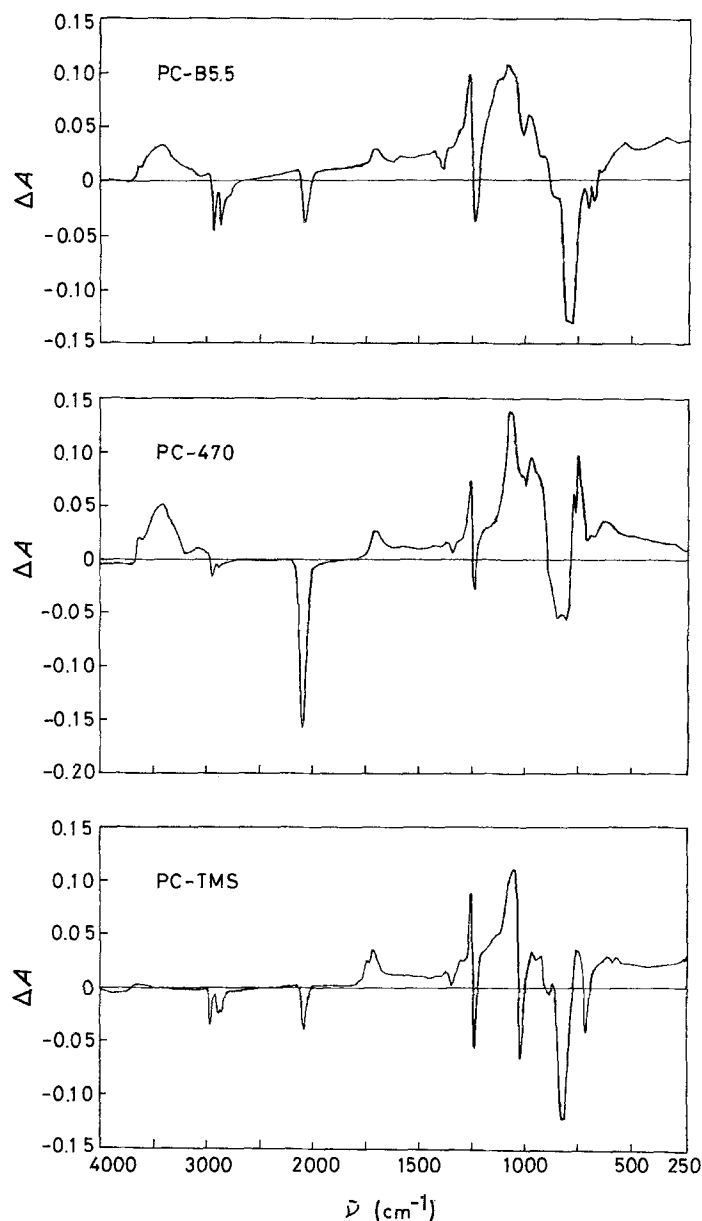
Figure 2 Infrared difference spectra of polycarbosilanes before and after curing.

where RH represents the PC. And then, ROH and a carbonyl group are formed by the following reactions

$$ROOH \rightarrow RO^{\cdot} + {^{\cdot}OH}$$

$$RO^{\cdot} + RH \rightarrow ROH + R^{\cdot}$$

$${^{\cdot}OH} + RH \rightarrow R^{\cdot} + H_2O$$

$$2ROO^{\cdot} \rightarrow \text{products containing } C{=}O + O_2.$$

The hydrogen atoms in RH exist in both the Si–H and C–H bonds. From Fig. 2, it is not clear which bond would be more reactive. Probably, the reactivity depends on the molecular structure. Furthermore, as shown in Fig. 1, the initiation temperatures of oxidation of each PC are different, and Table II and III show that the weight gains on curing do not correspond to the decrement of Si–H bond in Fig. 2. Thus,
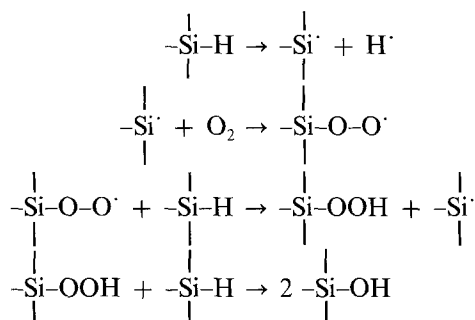
TABLE III Chemical compositions (wt %), empirical formulae of polycarbosilanes, the cured fibres and the heat-treated fibres at 1300°C in a vacuum

| PC	Si	C	H	O	B	Empirical formula
PC-TMS	44.8	39.9	6.79	1.21	–	$SiC_{2.08}H_{4.24}O_{0.047}$
Cured	–	–	–	10.5	–	
1300°C	50.6	35.6	–	12.5	–	$SiC_{1.64}O_{0.432}$
PC-470	48.2	39.9	6.85	0.81	–	$SiC_{1.77}H_{3.70}O_{0.035}$
Cured	44.4	31.0	5.30	5.11	–	$SiC_{1.63}H_{3.34}O_{0.201}$
1300°C	51.3	34.1	0.05	9.55	–	$SiC_{1.55}H_{0.027}O_{0.326}$
PC-B3.2	44.5	35.8	8.00	4.83	0.02	$SiC_{1.88}H_{5.03}O_{0.190}B_{0.001}$
Cured	41.0	31.0	6.97	15.9	–	$SiC_{1.76}H_{4.76}O_{0.679}$
1300°C	44.3	28.4	0.01	19.6	0.05	$SiC_{1.50}H_{0.006}O_{0.774}B_{0.003}$
PC-B5.5	44.9	39.2	7.44	3.56	0.06	$SiC_{2.04}H_{4.64}O_{0.139}B_{0.003}$
Cured	–	–	–	17.2	–	
1300°C	48.9	31.4	0.40	13.5	–	$SiC_{1.50}H_{0.229}O_{0.483}$

the mechanism of oxidation in PC may be more complicated.

3.1.1. Curing process of PC-470

In PC-470, it is clear that Si–H bonds are mainly oxidized and a small number of C–H bonds oxidized, as shown in Fig. 2. Consequently, the absorption peaks at 3650 and 3600 to 3200 cm^{-1} (the latter is affected by H_2O in KBr) should be assigned to O–H stretching vibration in the Si–OH bond. Thus, the main oxidation in PC-470 is assumed to be
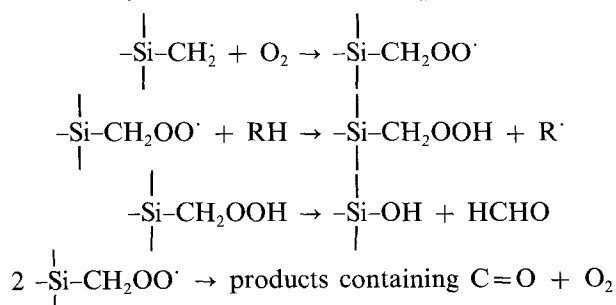
$$-\overset{|}{\underset{|}{Si}}-H \rightarrow -\overset{|}{\underset{|}{Si}}\cdot + H\cdot$$

$$-\overset{|}{\underset{|}{Si}}\cdot + O_2 \rightarrow -\overset{|}{\underset{|}{Si}}-O-O\cdot$$

$$-\overset{|}{\underset{|}{Si}}-O-O\cdot + -\overset{|}{\underset{|}{Si}}-H \rightarrow -\overset{|}{\underset{|}{Si}}-OOH + -\overset{|}{\underset{|}{Si}}\cdot$$

$$-\overset{|}{\underset{|}{Si}}-OOH + -\overset{|}{\underset{|}{Si}}-H \rightarrow 2 -\overset{|}{\underset{|}{Si}}-OH$$

Then, the silanol groups produced by the above reactions are dehydrated to form the siloxane bond

$$2 -\overset{|}{\underset{|}{Si}}-OH \xrightarrow{\Delta} -\overset{|}{\underset{|}{Si}}-O-\overset{|}{\underset{|}{Si}}- + H_2O$$
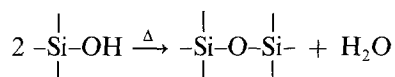
The details of these reactions will be reported in the near future. It was confirmed here that the initiation mechanism of thermal oxidation of PC-470 is the Si–H bond cleavage which occurs at about 100° C and significantly above 200° C, as suggested by the TG-DTA curve in Fig. 1.

3.1.2. Curing process of PC-TMS

It is distinct that in PC-TMS oxidation of the C–H bond is also predominant. Both C–H bonds in Si–CH$_3$ and Si–CH$_2$–Si seem to be oxidized. Under the curing conditions in Table II, Si–H bonds in PC-TMS should be oxidized by the same mechanism as PC-470. But, contrary to PC-470, no exothermic peak in the lower temperature range in the DTA curve of PC-TMS is observed. Further, in this study, it was observed that C=O bonds were formed and the oxygen content in PC-TMS increased as reported previously [1, 2] when PC-TMS is allowed to stand in contact with air at room temperature. These results show that the PC-TMS molecule has radical species such as $SI-CH_2^\cdot$ and Si–ĊH–Si. These radical species may remain because of the short reaction time between the pyrolysed tetramethylsilanes. Consequently, oxidation of PC-TMS is initiated by these radicals, for example

$$-\overset{|}{\underset{|}{Si}}-CH_2^\cdot + O_2 \rightarrow -\overset{|}{\underset{|}{Si}}-CH_2OO\cdot$$

$$-\overset{|}{\underset{|}{Si}}-CH_2OO\cdot + RH \rightarrow -\overset{|}{\underset{|}{Si}}-CH_2OOH + R\cdot$$

$$-\overset{|}{\underset{|}{Si}}-CH_2OOH \rightarrow -\overset{|}{\underset{|}{Si}}-OH + HCHO$$

$$2 -\overset{|}{\underset{|}{Si}}-CH_2OO\cdot \rightarrow products\ containing\ C=O + O_2$$

i.e. oxidation of PC-TMS begins at room temperature

and is not accompanied by a large weight gain if the methyl group is mainly oxidized to a silanol group. The weight gain on curing will be described later. By the above radical chain process, it is evident that the oxidation of the Si–H bond is initiated in a similar mechanism as for PC-470. The above process should also occur in PC-470 at high temperature.

3.1.3. Curing process of PC-B

PC-B is oxidized markedly at lower temperatures than PC-TMS and PC-470, as shown in Fig. 1. In DTA curves, both PC-B3.2 and PC-B5.5 have exothermic peaks at about 120° C. It has been reported that the higher the fraction of SiC_xSi_{4-x}, namely polysilane skeleton, in PC molecule, the lower is the curing temperature [3]. In this study, it was found that a sharp absorption peak appears at 1815 cm^{-1} when the infrared spectrum of PC-B is measured in CCl_4 solution. This peak is assigned to C=O stretching vibration in carbonyl chloride, $COCl_2$. Carbonyl chloride should be formed by the reaction between $\cdot CCl_3$ and dissolved oxygen in CCl_4. Silyl radical species produce $\cdot CCl_3$ from CCl_4 by the chlorine abstraction reaction [6]. The absorption peak at 1815 cm^{-1} does not appear in hexane solution and, without dissolved oxygen, it was confirmed that $CHCl_3$ is formed by the reaction between $\cdot CCl_3$ and Si–H [6]. Thus, it is evident that PC-B has silyl radical species in the molecule, and the oxidation is initiated by the radicals at room temperature

$$-\overset{|}{\underset{|}{Si}}\cdot + O_2 \rightarrow -\overset{|}{\underset{|}{Si}}-O-O\cdot$$
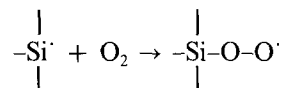
No silyl radical in PC-TMS is observed in the reaction with CCl_4.

At present, the formation mechanism of silyl radical species is not clear. In general the chlorine abstraction reaction of hydrosilanes from CCl_4 occurs in the presence of an initiator such as dibenzoyl peroxide. In contrast, hydropolysilanes such as pentamethyldisilane initiate the chlorine abstraction without initiator [7]. From the high concentration of SiC_xSi_{4-x} as shown in Table I, it is probable that hydrogen atoms bonded with silicon atoms forming the polysilane skeleton are present in PC-B. If this bond tends to be broken homolytically, silyl radical species are produced in PC-B. Carberry and West [8] observed that decamethylcyclopentasilane is oxidized readily in air at room temperature and a siloxane bond is formed. Another mechanism forming the silyl radical may be the cleavage of a strained ring containing a polysilane skeleton in PC-B.

In Fig. 2, C–H bonds in PC-B are oxidized more than PC-470. The reason is assumed to be that the concentration of methyl groups around the silyl radical in PC-B is much higher than that in PC-470.

3.1.4. Structure of cured polycarbosilane

To examine the pyrolysis process of cured PC fibre, the structure of cured PC should be determined in a similar manner as is shown in Table I.

The decrement of Si–H bonds on oxidation, i.e. $SiC_3H \rightarrow SiC_3O$, can be determined from the decrement
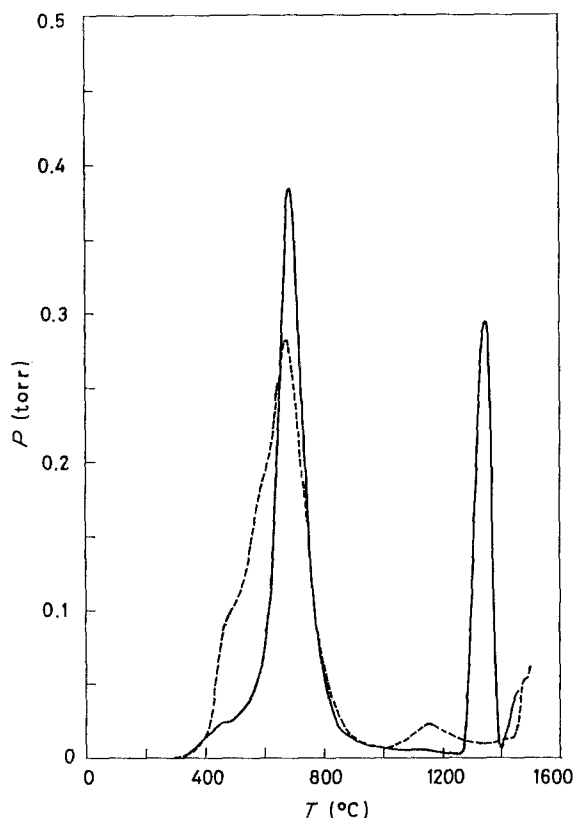
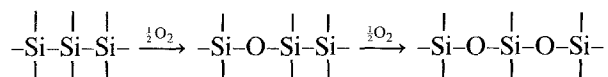*Figure 3* Gas evolution curves of PC-B5.5 ($\cdots$) before and (——) after curing.

of absorbance of the absorption peak at $2100\,\mathrm{cm}^{-1}$ in the infrared spectrum. The results of the determinations are shown in Table IV.

For the oxidation of the C–H bond, a simplifying assumption can be made without leading to serious errors: only methyl groups are oxidized to give silanol groups or siloxane bonds. After curing, the formation of the silanol group gives little weight gain and formation of the siloxane bond produces a weight loss in the PC fibre. On this assumption, the proportions of oxidized methyl groups in PC-TMS, PC-470, PC-B3.2 and PC-B5.5 are 23, 15, 28 and 25%, respectively. These values were calculated from the absorbance of the peak at $2950\,\mathrm{cm}^{-1}$ in the infrared spectra.

In spite of the smaller fraction of SiC_3O in PC-B than in PC-470 as shown in Table IV, the weight gain of PC-B after curing is much larger than of PC-470, as shown in Table II, because the silicon atom represented by SiC_xSi_{4-x} is easily oxidized
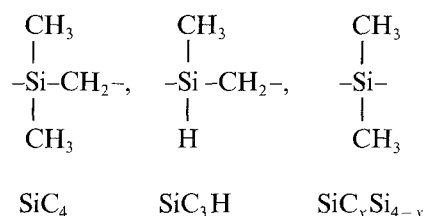
$$SiC_xSi_{4-x} \rightarrow SiC_xSi_{4-x-1}O \rightarrow SiC_xSi_{4-x-2}O_2 \rightarrow \cdots$$
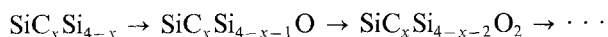
If the linear polysilane skeleton is assumed, the linear siloxane bonds are formed

$$-\overset{|}{\underset{|}{Si}}-\overset{|}{\underset{|}{Si}}-\overset{|}{\underset{|}{Si}}- \xrightarrow{\frac{1}{2}O_2} -\overset{|}{\underset{|}{Si}}-O-\overset{|}{\underset{|}{Si}}-\overset{|}{\underset{|}{Si}}- \xrightarrow{\frac{1}{2}O_2} -\overset{|}{\underset{|}{Si}}-O-\overset{|}{\underset{|}{Si}}-O-\overset{|}{\underset{|}{Si}}-$$
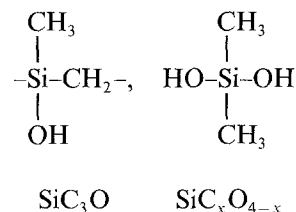
The proportion of oxidized polysilane skeleton can be estimated from the amounts of the first gas evolution which occurs during pyrolysis of the polysilane skeleton in PC-B [2]. The gas evolution curves of PC-B5.5 before and after curing are shown in Fig. 3. These curves show that the amounts of the first gas evolution in the temperature range 300 to 600° C is much decreased by curing. The decrement is determined by subtracting the area of the first gas evolution

peak after curing (subtract the peak area of PC-470 from the peak area of PC-B) from the area of the first gas evolution peak before curing (subtract the peak area of PC-470 from the peak area of PC-B). Thus, it was determined that the proportions of residual polysilane skeleton in PC-B3.2 and PC-B5.5 after curing are 22.8 and 29.7% respectively. Characterization of siloxane bonds is examined using nuclear magnetic resonance (NMR). In this report, as structural elements in cured PC-B, silicon atoms forming the partially oxidized polysilane skeleton were separated into two elements: SiC_xSi_{4-x} for the residual polysilane skeleton and SiC_xO_{4-x} for the perfectly oxidized polysilane skeleton.
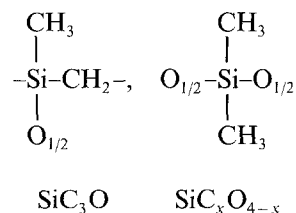
When the structure of cured PC is discussed, one of the most important subjects is whether the oxygen introduced by curing into PC is in the silanol group or the siloxane bond. If the following structural elements for SiC_4, SiC_3H and SiC_xSi_{4-x} in Table I are assumed

$$
\begin{array}{ccc}
\mathrm{CH_3} & \mathrm{CH_3} & \mathrm{CH_3} \\
| & | & | \\
-\mathrm{Si}-\mathrm{CH_2}-, & -\mathrm{Si}-\mathrm{CH_2}-, & -\mathrm{Si}- \\
| & | & | \\
\mathrm{CH_3} & \mathrm{H} & \mathrm{CH_3} \\
\end{array}
$$

$$
\begin{array}{ccc}
SiC_4 & SiC_3H & SiC_xSi_{4-x}
\end{array}
$$

and the average number of methyl groups bonded with one silicon atom in PC-TMS, PC-470, PC-B3.2 and PC-B5.5 is 1.61, 1.22, 1.42 and 1.23 [2], the molecular weight of a silicon atom, M_0, in each PC is given as shown in Table I. Then, using the following structural elements for SiC_3O and SiC_xO_{4-x},

$$
\begin{array}{cc}
\mathrm{CH_3} & \mathrm{CH_3} \\
| & | \\
-\mathrm{Si}-\mathrm{CH_2}-, & \mathrm{HO}-\mathrm{Si}-\mathrm{OH} \\
| & | \\
\mathrm{OH} & \mathrm{CH_3} \\
\end{array}
$$

$$
\begin{array}{cc}
SiC_3O & SiC_xO_{4-x}
\end{array}
$$

and silanol groups formed by partial oxidation of methyl groups, $Si–CH_3 \rightarrow Si–OH$, the average molecular weight, M_1, is given as shown in Table IV. On the other hand, if all silanol groups form siloxane bonds on dehydration

$$
\begin{array}{cc}
\mathrm{CH_3} & \mathrm{CH_3} \\
| & | \\
-\mathrm{Si}-\mathrm{CH_2}-, & \mathrm{O_{1/2}}-\mathrm{Si}-\mathrm{O_{1/2}} \\
| & | \\
\mathrm{O_{1/2}} & \mathrm{CH_3} \\
\end{array}
$$

$$
\begin{array}{cc}
SiC_3O & SiC_xO_{4-x}
\end{array}
$$

the average molecular weight, M_2, also is given as shown in Table IV.

Using M_0 and M_1 or M_2, the weight gain of PC on curing can be calculated for PC-TMS, PC-470, PC-B3.2 and PC-B5.5: using M_1, 3.5, 5.6, 24.4 and 21.8%, respectively; using M_2, -2.9, 0, 5.8 and 5.7%, respectively. These results in comparison with the weight gains in Table II, show the effectiveness of M_1 for PC-TMS and PC-470, and the ineffectiveness of both M_1 and M_2 for PC-B, which is due to the presence of both states of the silanol group and siloxane bond in
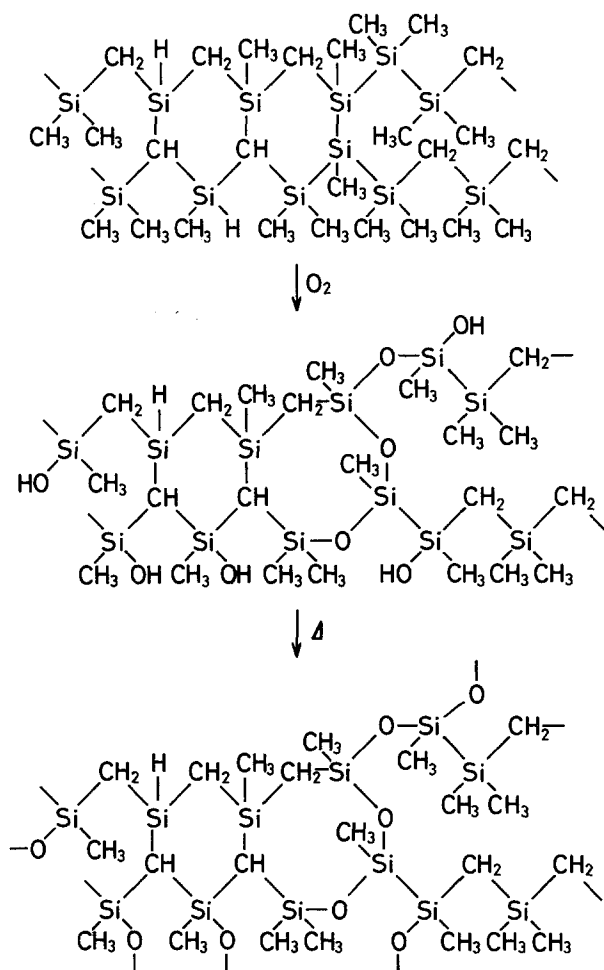
Figure 4 A curing mechanism of polycarbosilane.

Figure 5 TG-DTA curves of cured polycarbosilane fibres in a nitrogen flow.

cured PC-B. Perhaps it should be assumed that the oxidized polysilane skeleton produced siloxane bonds, because no decrease in the molecular weight of PC-B by scission of the chain was observed. Thus, in calculation of M_1, assuming SiC_xO_{4-x} consists of siloxane bonds, the corrected values of M_1 of PC-B3.2 and PC-B5.5 are 64.7 and 60.8, respectively, in good agreement with the measured values. From the above results, the oxygen contents of cured PC-TMS, PC-470, PC-B3.2 and PC-B5.5 are calculated to be 10.8, 9.3, 20.8 and 17.9 wt%, respectively, in agreement with the values given in Table III.

From the above results, it seems remarkable to assume that some part of the Si–H bonds and Si–CH$_3$ bonds in PC are oxidized to give Si–OH bonds and to become infusible by dehydration between the silanol groups, i.e. cross-linking between PC molecules. From
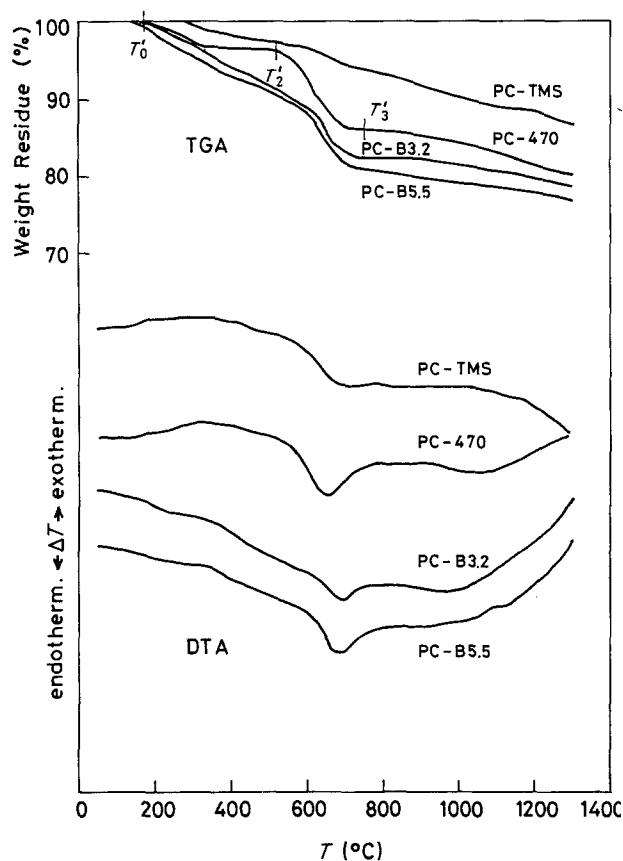
calculation of weight gain by M_0 and M_1, the concentration of cross-linking should be very low. On the other hand, the oxidized polysilane skeleton in PC-B should make localized siloxane bonds. In Fig. 4, the oxidation and cross-linking process in the curing of PC-B is shown.

Although there are some problems in determining the average number of methyl groups and oxidizing them, and in the characterization of other side chains or bonds containing oxygen formed, the structure presented for cured PC can explain satisfactorily the pyrolysis process.

3.2. Characterization of pyrolysis process of cured polycarbosilane fibre

The pyrolysis process of cured PC fibre is divided into some stages by TG-DTA curves and gas evolution curves in a similar manner as PC before curing [1].

The TG-DTA curves of cured PC fibres in a nitrogen flow are shown in Fig. 5. The weight residues of

TABLE IV Fractions* of SiC_4, SiC_3H, SiC_3O, SiC_xSi_{4-x} and SiC_xO_{4-x} and M_1 and M_2† of cured polycarbosilane

PC	SiC_4	SiC_3H	SiC_3O	SiC_xSi_{4-x}	SiC_xO_{4-x}	M_1	M_2
PC-TMS	0.82	0.09	0.09	0	0	68.3	64.2
PC-470	0.53	0.28	0.19	0	0	63.9	60.5
PC-B3.2	0.40	0.06	0.10	0.10	0.34	70.8 (64.7)	60.2
PC-B5.5	0.44	0.07	0.08	0.12	0.29	66.0 (60.8)	57.3

* By curing, the percentages of oxidized methyl groups in these structural elements are found to be 23, 15, 28 and 25% for PC-TMS, PC-470, PC-B3.2 and PC-B5.5, respectively.

† Both M_1 and M_2 are average molecular weights of a silicon atom based on the following assumptions: for M_1, all oxygen atoms in silanol groups; for M_2, all oxygen atoms in siloxane bonds. (M_1) is M_1 corrected by the assumption that oxygen atoms in SiC_xO_{4-x} are in siloxane bonds.
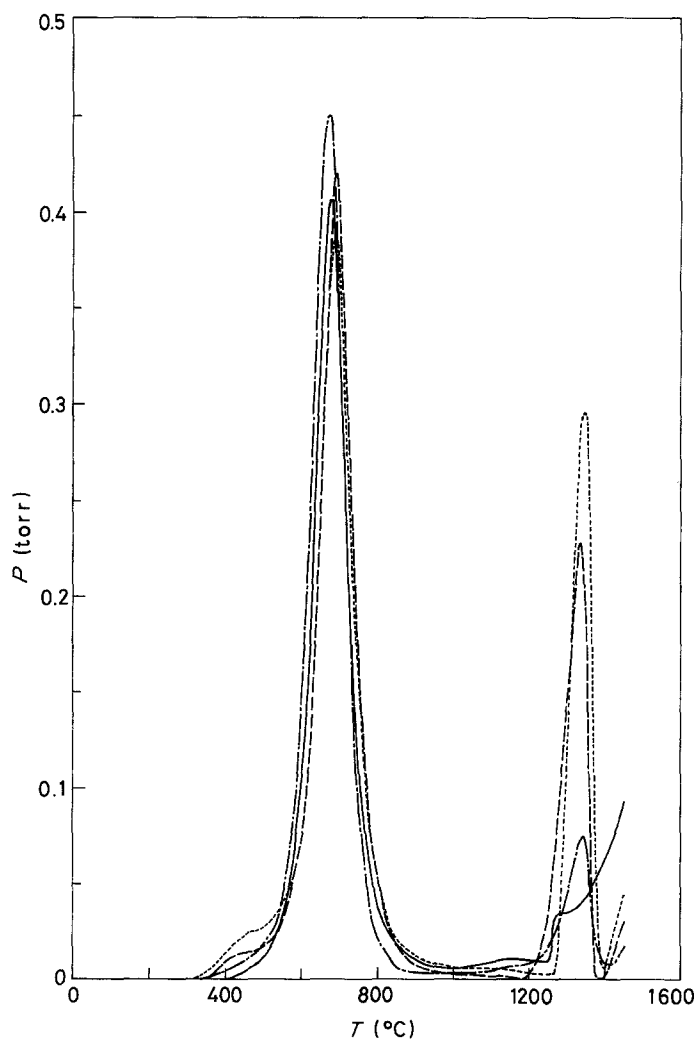
Figure 6 Gas evolution curves of cured polycarbosilane fibres in the pyrolysis process. (——) PC-TMS, (---) PC-470, (— — —) PC-B3.2, (- - -) PC-B5.5.

cured PC fibres at 1300° C are higher than those of PCs before curing by 15 to 20%. The TG-DTA curves have the same endothermic peaks centred at 650 to 700° C as uncured PCs, but no exothermic peaks centred at 1020° C are observed in uncured PC-TMS and PC-470. In the TGA curves, the initiation and termination temperatures of rapid weight loss corresponding to the endothermic peak in the DTA curve are represented by T_2' and T_3', respectively, and the initiation temperature of weight loss by T_0'. In the range of T_2' to T_3', it is evident that pyrolysis of the side chains similar to uncured PC mainly occurs [1]. Curing considerably reduces the weight loss in the range T_0' to T_2' and has no effect on the weight loss between T_2' and 1300° C, compared with uncured PC.

The gas evolution of cured PC fibre during pyrolysis shown in Fig. 6 is divided into four stages: the first gas evolution observed in PC-B in the range 400 to 500° C; the second observed in all PCs in the range 500 to 800° C; the third in the range from 1200 to 1400° C; the fourth above 1400° C. The first gas evolution is due to the presence of the polysilane skeleton in cured PC-B fibre. The second gas evolution corresponding to the endothermic peak in DTA curve in Fig. 5 is due to hydrogen and methane produced by decomposition of the side chains in cured PC fibre. The most striking characteristic of gas evolution of cured PC fibre is the ocurrence of the third gas evolution peak centred at 1300° C, as shown in PC-B5.5 before and after curing in Fig. 3. Further, no gas evolution peak in the

temperature range 1000 to 1200° C is observed. The initiation and termination temperatures of the third gas evolution are represented by T_{4-1}' and T_{4-2}', respectively.

It was found that the pyrolysis process of cured PC can be discussed with the divisions at temperature T_0', T_2', T_3', T_{4-1}' and T_{4-2}', as in Table V. There are thus five stages in the pyrolysis process: up to T_2', T_2' to T_3', T_3' to T_{4-1}', T_{4-1}' to T_{4-2}', and above T_{4-2}'. The conversion mechanism into the inorganic state by pyrolysis and the structure of the product in each stage will be discussed.

3.2.1. The first stage up to 550° C

The first stage up to T_2' of the pyrolysis process will be discussed. In this temperature range, a large weight loss due to evaporation of low molecular weight PC and polymerization occurred in the case of PC before curing [1]. The pyrolysis of the polysilane skeleton occurred in PC-B [1]. However, in cured PC fibres the weight losses are very small. This shows that PC is

TABLE V Temperatures (° C) dividing the pyrolysis process of cured polycarbosilanes

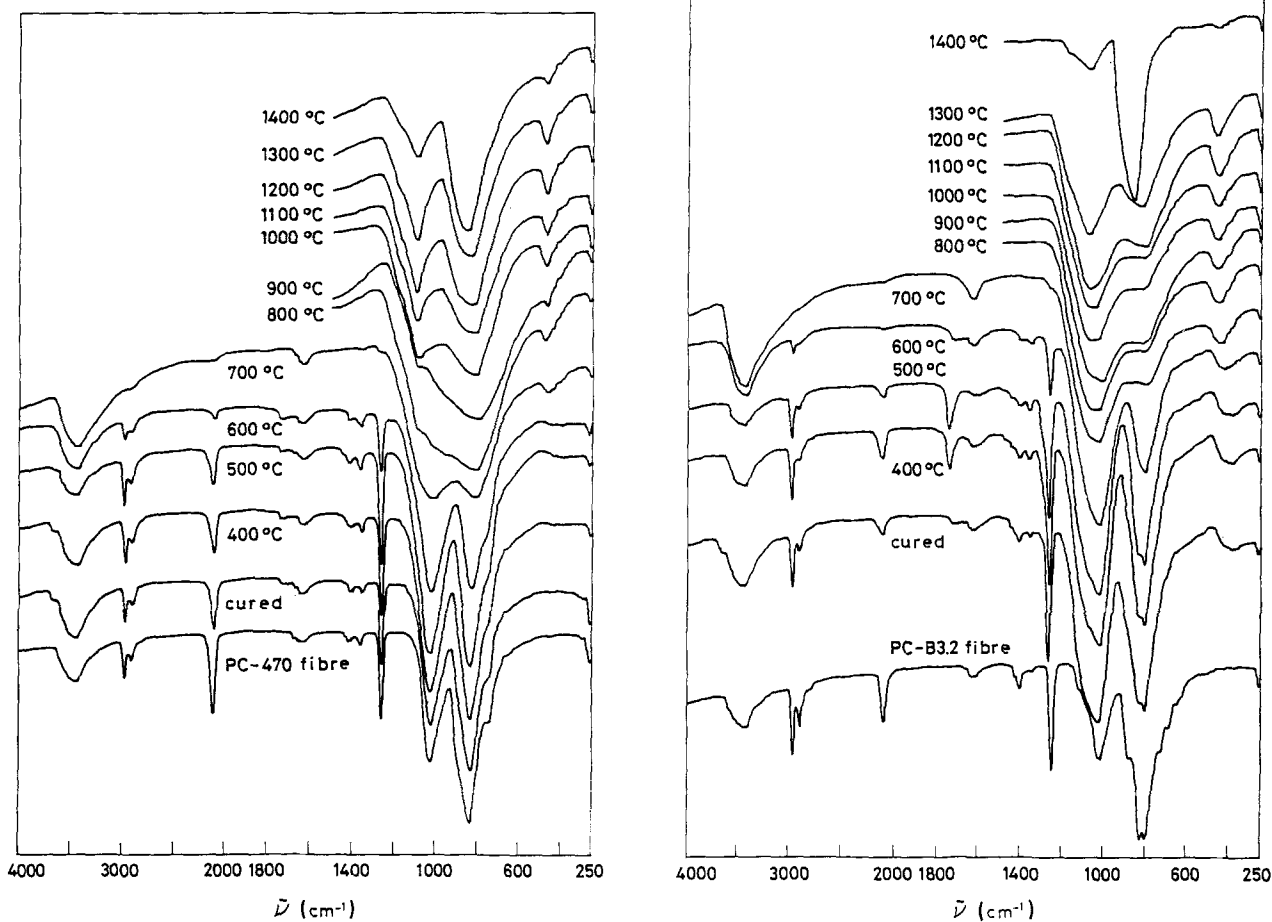| PC	T_0'	T_2'	T_3'	T_{4-1}'	T_{4-2}'
PC-TMS	280	580	720	1250	1370
PC-470	170	520	750	1200	1420
PC-B3.2	160	540	740	1190	1380
PC-B5.5	140	530	730	1270	1400

Figure 7 Infrared spectra of cured PC-470 and PC-B3.2 fibres heat treated in the range 400 to 1400° C in a vacuum.

cross-linked by curing. Up to T_2', the weight losses of cured PC-TMS, PC-470, PC-B3.2 and PC-B5.5 are 3.0, 3.6, 11.5 and 11.8%, respectively, which is discussed next.

The changes in infrared spectra of PC-470 and PC-B3.2 fibres on heat-treatment are shown in Fig. 7. PC-TMS and PC-B5.5 showed similar changes in the infrared spectra of PC-470 and PC-B3.2, respectively. From these infrared spectra, the change of the ratios of absorbances of the peaks at $2100 \, cm^{-1}$ (Si–H stretching), $1350 \, cm^{-1}$ (CH_2 deformation in Si–CH_2–Si) and $1250 \, cm^{-1}$ (Si–CH_3 deformation) to absorbance of the peak at $2950 \, cm^{-1}$ (C–H stretching), A_{2100}/A_{2950}, A_{1350}/A_{2950} and A_{1250}/A_{2950}, with heat-treatment are shown in Fig. 8. As can be seen from the comparison with uncured PC [1], the increases of A_{1350}/A_{2950} and A_{1250}/A_{2950} in PC-B are smaller and the decrease of A_{2100}/A_{2950} in all PCs seems to occur at lower temperature. The former is due to the small residue of polysilane skeleton in cured PC-B, and the latter should be due to dehydrogenation or demethanation caused by Si–H bond cleavage. However, the mechanism of Si–H cleavage is not clear because the gas evolution is small in this stage as shown in Fig. 6. The details are now being examined.

On the other hand, it is apparent from Table IV that in cured PC the number of silanol groups is larger than that of Si–H bonds: 1.3 times in PC-470 and about 5 times in the other PCs. Consequently, it is probable that siloxane bonds are mainly formed by the dehydration between silanol groups. From examination of

the peak at 3200 to $3650 \, cm^{-1}$ in the infrared spectrum, it has become apparent recently that Si–OH bonds disappear up to about 450° C. In the spectra in Fig. 7, this fact is hidden by H_2O in the KBr disc. By use of M_1 or modified M_1 and M_2 in Table IV, the weight losses by dehydration between silanol groups forming siloxane bonds are found to be 6.0% for PC-TMS, 5.3% for PC-470, 7.0% for PC-B3.2 and 5.8% for PC-B5.5 which are close to the observed values in TGA curves up to T_2'.

From the results presented above, in the first stage up to 550° C in the pyrolysis process, siloxane bonds are formed and cross-linking proceeds by dehydration between silanol groups, as shown in Fig. 4.

3.2.2. The second stage from 550 to 750° C

In the second stage T_2' to T_3', the decomposition of the side chains such as Si–H and Si–CH_3 occurs. This is evident from similar TG-DTA curves, gas evolution and infrared spectra as for PC before curing [1].

The characteristic change in this stage is the rapid increase in the density of the fibre at 600 to 700° C as shown in Fig. 9, corresponding to the disappearance of the peaks at 2950 and $2910 \, cm^{-1}$ (C–H stretching), $2100 \, cm^{-1}$ (Si–H stretching), $1350 \, cm^{-1}$ (CH_2 deformation in Si–CH_2–Si) and $1250 \, cm^{-1}$ (Si–CH_3 deformation) in the infrared spectra in Fig. 7. By the decomposition of side chains, PC is converted into the inorganic structure with a network and three-dimensional structure. The cured PC fibres are converted into the inorganic state via the solid-phase
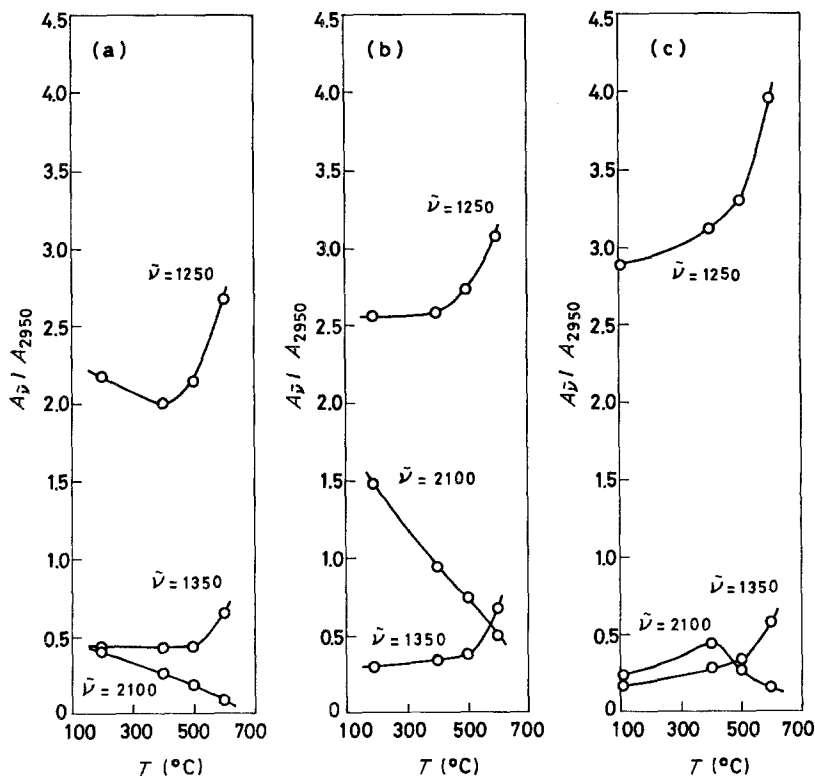
Figure 8 Changes in $A_{\tilde{\nu}}/A_{2950}$ of cured poly-carbosilane fibres during heat treatment: (a) PC-TMS; (b) PC-470; (c) PC-B3.2.

reaction and have many oxygen atoms around the original PC molecule. Therefore, the structure of the product obtained in the second stage is disordered, such as is shown in Fig. 10, and the growth of the SiC skeleton is depressed.

In the second stage, the cured PC fibres are converted into inorganic structure by the decomposition of Si–H and C–H in Si–CH$_3$ and Si–CH$_2$–Si bonds, such as dehydrogenation and demethanation, and rapidly increase the density.

3.2.3. The third stage from 750 to 1200° C

In the third stage from T_3' to T_{4-1}', gas evolution by
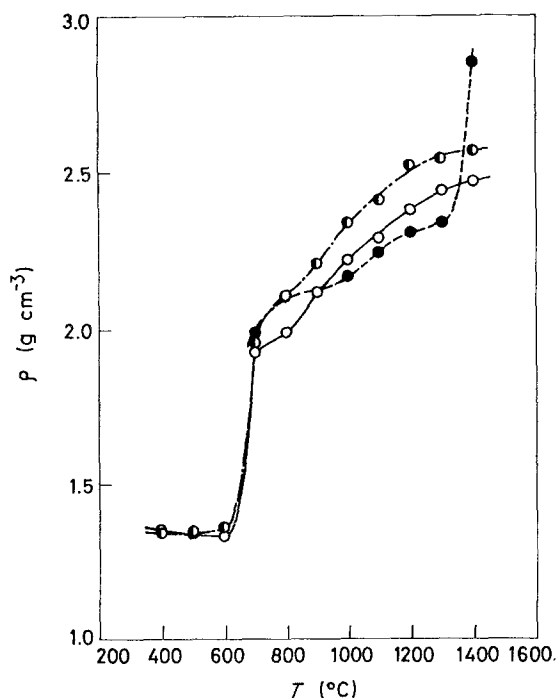
Figure 9 Densities of cured polycarbosilane fibres heat treated in a vacuum. (O) PC-TMS, (◐) PC-470, (●) PC-B3.2.

pyrolysis is almost complete, the stage proceeds to the next stage of gas evolution.

Infrared spectra at 800° C in Fig. 7 show peaks in the bands of 820 cm^{-1} (Si–C stretching), 1020 cm^{-1} (CH$_2$ wagging in Si–CH$_2$–Si) and 460 cm^{-1} (Si–O–Si deformation), and the peak in the band of 1020 cm^{-1} shifts to 1080 cm^{-1} (Si–O stretching) with increasing temperature. The density of the fibre also increases with heat-treatment temperature as shown in Fig. 9. These results show that the conversion of PC fibre into the inorganic fibre is completed with increasing temperature.

In this stage the most characteristic feature of pyrolysis of cured PC fibres is the absence of a gas evolution peak in the range 1000 to 1200° C which was observed as dehydrogenation in uncured PC. In the pyrolysis product of uncured PC, the first β-SiC crystallization occurred by dehydrogenation [1].

The X-ray powder diffraction patterns of cured PC fibres heat treated at 900° C or above are shown in Fig. 11. The separation of the diffraction peaks (2 2 0) and (3 1 1) of β-SiC is not distinct below 1200° C in any PC, so that the products should be in the amorphous state. In particular, in PC-B the diffraction peaks of β-SiC are broad even at 1300° C. The apparent crystalline size L_{111} was calculated from the half-width β of the (1 1 1) line of the β-SiC, using Scherrer's formula
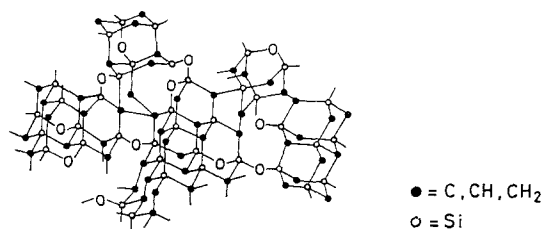

● = C, CH, CH$_2$
o = Si

Figure 10 Presumed structure of cured polycarbosilane fibre in the course of the pyrolysis process.

(a)

900 °C

1000 °C

1100 °C

1200 °C

1300 °C

1400 °C (x 0.8)

10   20   30   40   50   60   70   80   90   100

2θ (Cu $K\alpha$)

(b)

900 °C

1000 °C

1100 °C

1200 °C

1300 °C

1400 °C

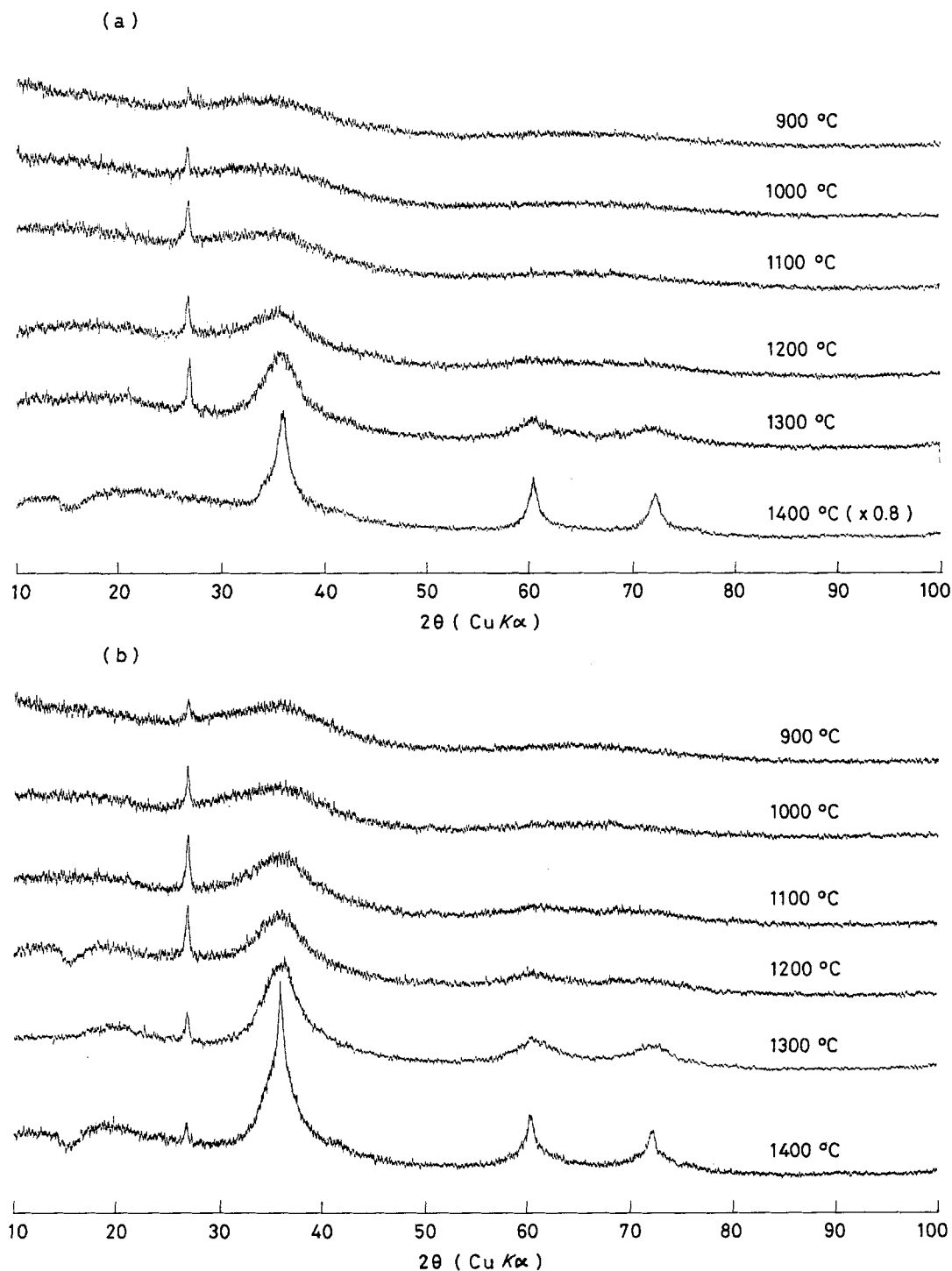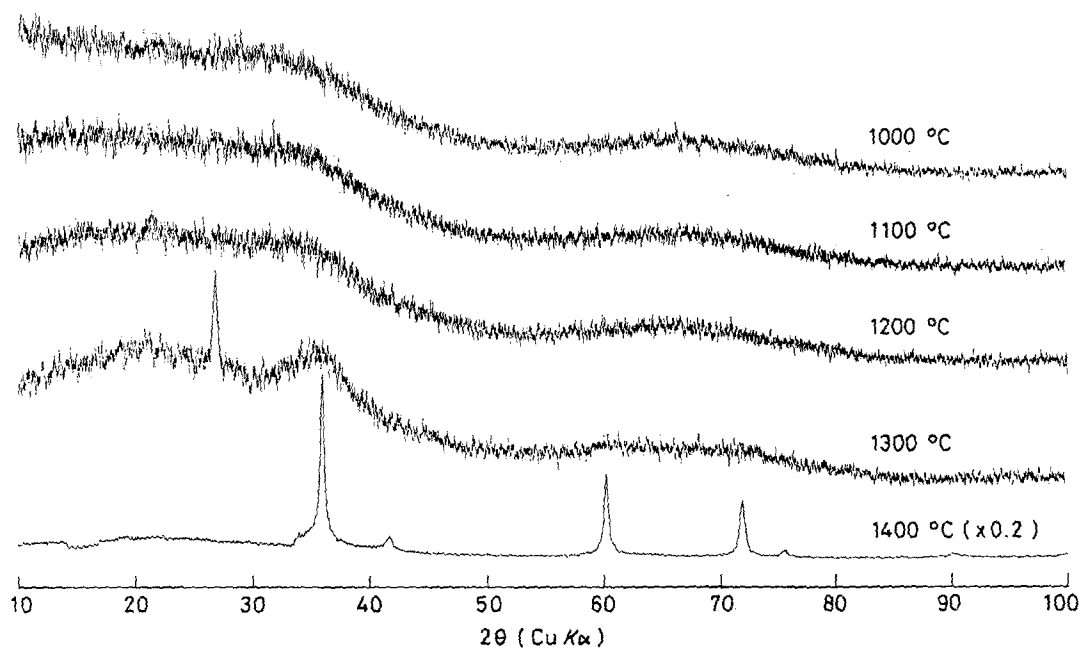10   20   30   40   50   60   70   80   90   100

2θ (Cu $K\alpha$)

Figure 11 X-ray diffraction patterns of cured polycarbosilane fibres heat treated in a vacuum: (a) PC-TMS; (b) PC-470; (c) PC-B3.2; (d) PC-B5.5.

$L_{111} = 1.0\lambda/(\beta \cos \theta)$ where λ is the wavelength of X-rays and θ the diffraction angle. The relationship between L_{111} and heat-treatment temperature in PC-TMS and PC-470 is shown in Fig. 12, where L_{111} for uncured PC is shown [1]. The crystalline sizes of cured PC-TMS at 1000° C and of cured PC-470 at 900° C are the same as that of the uncured specimens. However, in spite of increasing heat-treatment temperature, the first β-SiC crystallization in cured PC fibre does not occur. Therefore, the crystalline size of cured PC fibre heat treated to 1300° C is smaller than that of uncured PC. The cause of the depressed crystallization of β-SiC seems to be oxygen introduced into the fibre in the curing process. That is, the oxygen present as cross-linking in Fig. 10 inhibits the growth of SiC grains

with a molecular size of the original PC. The relationship between the molecular size of the original PC and the SiC grain size is discussed below in some detail.

As in Table I, the number average molecular weight of PC increases in the order PC-TMS < PC-B5.5 < PC-B3.2 < PC-470. However, PC-B has a polysilane skeleton which can be easily oxidized in the molecule. So, the molecular weight of the continuous carbosilane skeleton in the cured PC-B should be defined as the available molecular weight: the available molecular weight of PC-B being smaller than the number average molecular weight. From Table I the molecular weights of the polysilane skeleton, if PC-B has localized $SiC_x Si_{4-x}$, are 690 for PC-B3.2 and 475 for PC-B5.5. After curing, the molecular weights of the residual

1000 °C

1100 °C

1200 °C

1300 °C

1400 °C (x0.2)

2θ (Cu Kα)

(d)

1000 °C

1100 °C
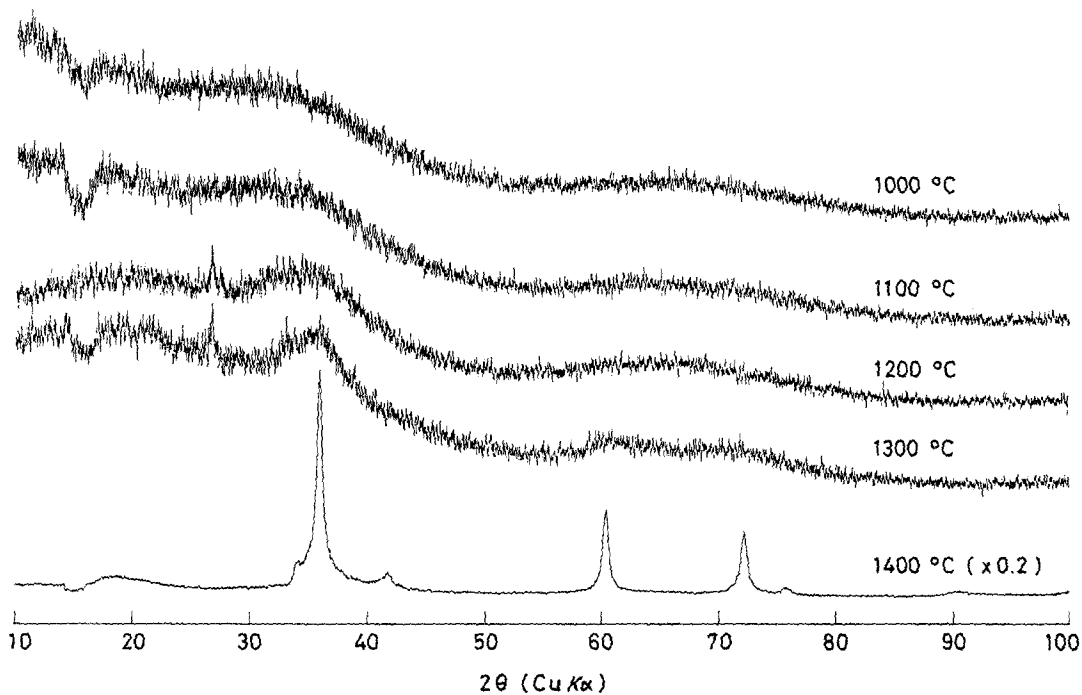
1200 °C

1300 °C
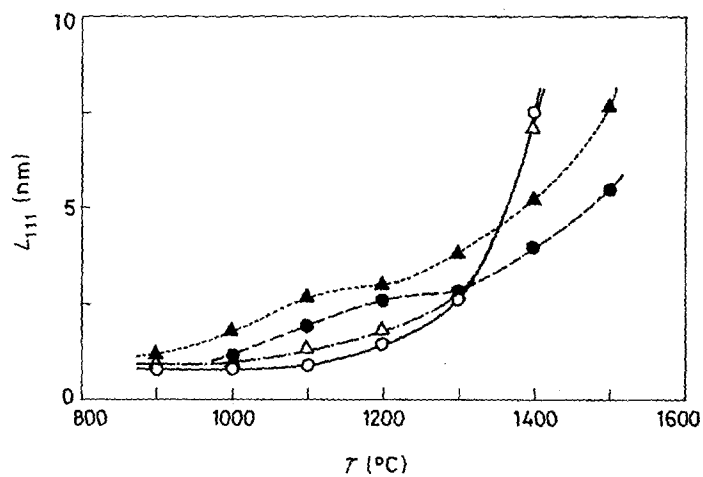
1400 °C (x0.2)

2θ (Cu Kα)

Figure 11 Continued

Figure 12 Apparent crystalline sizes of β-SiC (L_{111}) in polycarbosilanes heat-treated in a vacuum before (●, ▲) and after (○, △) curing. (○, ●) PC-TMS, (△, ▲) PC-470.
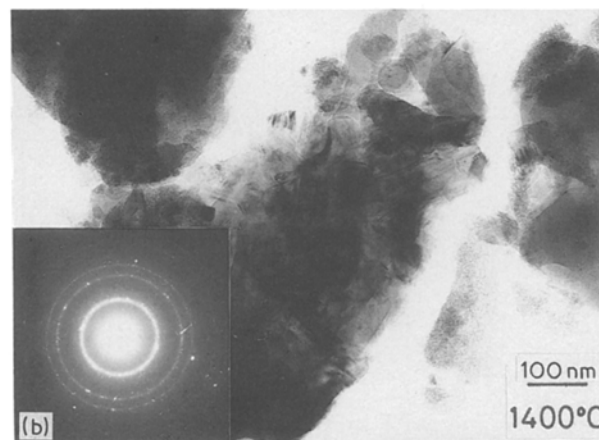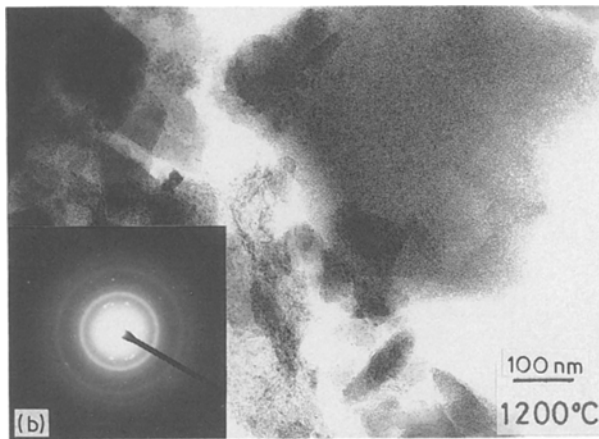
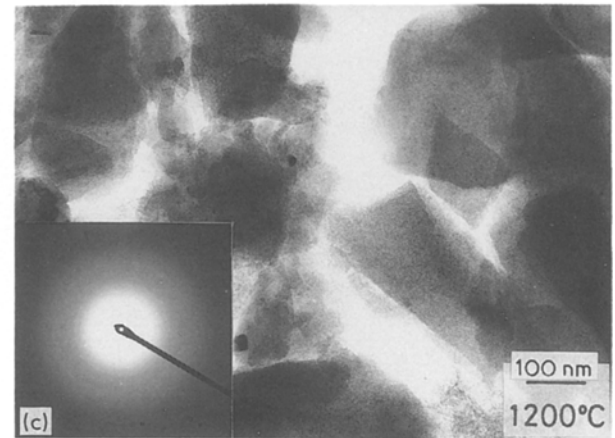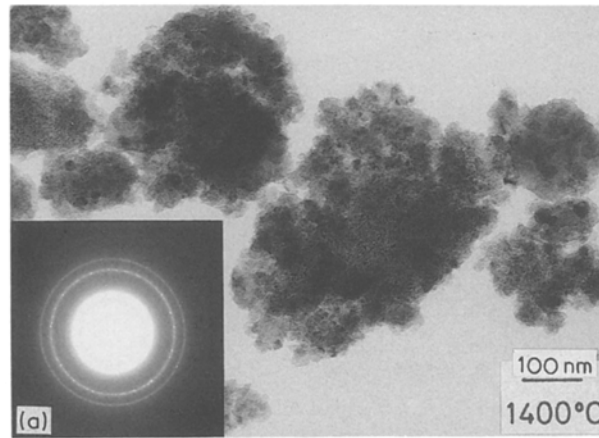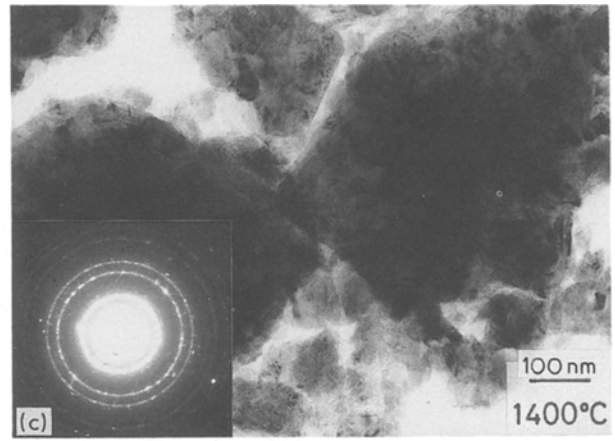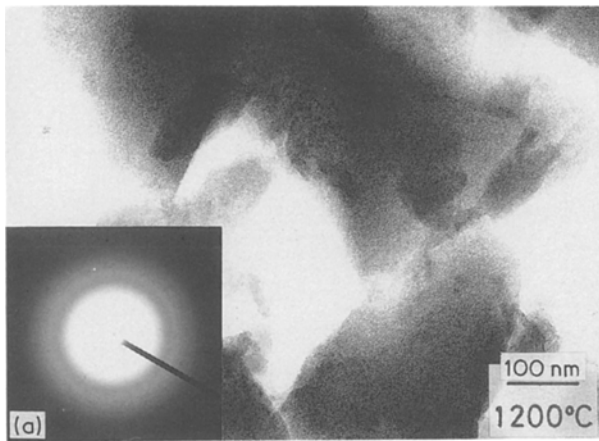L_{111} (nm)

T (°C)

Figure 13 Bright-field transmission electron micrographs and selected-area diffraction patterns for cured (a) PC-TMS, (b) PC-470 and (c) PC-B3.2 fibres obtained at 1200 and 1400° C.

localized siloxane bonds in PC-B are shown in Fig. 4. The number average molecular weight of PC-TMS increased to 1340 during spinning, because PC-TMS increased in molecular weight on heat treatment [1].

From the above discussion, the available molecular weight of carbosilane and polysilane skeleton consisting of cured PC fibre increases in the order PC-B5.5 (490) < PC-B3.2 (600) < PC-TMS (1340) < PC-470 (1740). PC-470 of molecular weight 1740 has 29 Si atoms using $M_0 = 60.5$ in Table I, corresponding to a grain of about 1.5 nm diameter. The grain sizes of PC-TMS, PC-B3.2 and PC-B5.5 are 1.2, 0.5 and 0.4 nm, respectively, using available molecular weights. These values for PC-470 and PC-TMS are in agreement with L_{111} in the temperature range 1100 to 1200° C in Fig. 12. The X-ray diffraction patterns of PC-B fibre in Fig. 11 are also in agreement with those expected from the available molecular weights.

Thus, SiC grains with a size corresponding to the available molecular weight of the original PC are formed in the fibre and grain growth is depressed by oxygen atoms existing between the grains. The dehydrogenation accompanying crystallization in uncured PC is hardly observed. That is, it indicates that the hydrogen concentration in the grain boundary is very low.

In the third stage, the gas evolution is small and the density of the product increases. The structure of the fibre is amorphous and the apparent β-SiC crystalline sizes are 1.2 to 1.5 nm in PC-TMS and PC-470 and 0.4

polysilane skeletons are 157 for PC-B3.2 and 139 for PC-B5.5 (Table IV). Therefore, the total molecular weights of carbosilane and polysilane skeleton after curing are 1207/2 for PC-B3.2 and 974/2 for PC-B5.5;
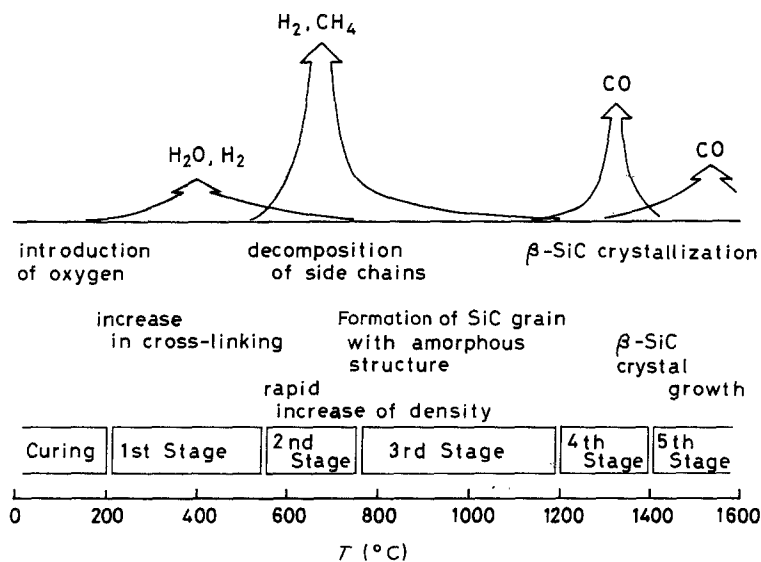
Figure 14 Conversion process of cured polycarbosilane fibres into the inorganic fibre by pyrolysis.

to 0.5 nm in PC-B, depending on the available molecular weights of the original PCs. The oxygen atoms introduced into the fibre by curing, depress the crystallization of β-SiC.

3.2.4. The fourth stage from 1200 to 1400°C

In the fourth stage from T'_{4-1} to T'_{4-2}, there again appears a gas evolution peak, as shown in Fig. 6. The gas is CO [9]. The temperature range of this gas evolution, as shown in Fig. 3, is higher than that of dehydrogenation in the fifth stage in uncured PC and can be distinguished from the gas evolution above 1400°C. Therefore, the gas evolution in this stage is characteristic of cured PC fibre.

The areas of the gas evolution peaks in the fourth stage in PC-B3.2 and PC-B5.5 fibres are 3.21 and 3.47 times that in PC-470, respectively. These areas seem to be proportional to the oxygen content in M_2 in Table IV: 5.7, 4.9, 15.7 and 13.5 wt % in PC-TMS, PC-470, PC-B3.2 and PC-B5.5, respectively. The gas evolution should be caused by the oxygen introduced by curing.

The transmission electron micrographs and their corresponding electron diffraction ring patterns of PC-TMS, PC-470 and PC-B3.2 fibres obtained at 1200 and 1400°C are shown in Fig. 13. These TEM observations show the considerable β-SiC crystallization in the fourth stage, in agreement with Figs 11 and 12. From the decrease of the peak intensities at 1080 cm^{-1} (Si–O stretching) in the infrared spectra in Fig. 7, and the increase of the density of PC-B fibre in Fig. 9, it is clear that the reaction between Si–O bonds and excess carbon has been completed at 1400°C. When the empirical formula of cured PC fibre obtained at 1300°C is represented by $SiC_{1+a}O_{a+b}$ from Table III, the values of b are -0.21, -0.22, 0.27 and -0.02 for PC-TMS, PC-470, PC-B3.2 and PC-B5.5, respectively. From these b values, in PC-TMS and PC-470 the excess carbon seems to remain in the fibres at 1400°C. On the other hand, excess oxygen in PC-B3.2 is regarded as volatile SiO at 1400°C in vacuum. The densities of PC-TMS and PC-470 fibres hardly increase owing to the residual excess of carbon. Consequently, the amount of β-SiC produced in

reduction of the Si–O bonds in PC-TMS and PC-470 should be lower than that in PC-B. This is supported by L_{111} at 1400°C obtained from Fig. 11, in the order of PC-470 (7.1 nm) < PC-TMS (7.6 nm) < PC-B5.5 (16.3 nm) < PC-B3.2 (22.6 nm).

In the fourth stage, the rapid crystal growth of β-SiC grains with a size corresponding to the available molecular weight of PC, results from reaction between the Si–O bond and excess carbon in the grain boundary. The degree of crystal growth is closely related to the amount of oxygen introduced by curing.

3.2.5. The fifth stage above 1400°C

In the fifth stage above T'_{4-2} there again appears a gas evolution, as shown in Fig. 6. The gas is again CO and is observed in the case of uncured PC [1]. Perhaps a reaction between residual oxygen and excess carbon or SiC [10] occurs and L_{111} increases.

4. Conclusion

In each PC, the silicon atoms forming the cured PC skeleton are represented by means of five simple elements. It has been shown that some of the methyl groups were oxidized to give silanol groups. The curing mechanism is cross-linking between PC molecules by dehydration between silanol groups, resulting from oxidation of Si–H and Si–CH$_3$.

The conversion process of cured PC fibre into silicon carbide fibre can be divided into five temperature ranges. The structures of the pyrolysis products in each stage have been studied. The following results are also summarized in Fig. 14.

In the first stage, the concentration of cross-linking increases by dehydration between the silanol groups in cured PC fibres. There is virtually no weight loss due to vaporization of low molecular weight PC.

In the second stage, by decomposition of the side chains of PC, such as dehydrogenation and demethanation, cured PC is converted into the inorganic structure with a large gas evolution and the density of the fibre increases rapidly. Oxygen atoms form cross-links between the grains.

In the third stage, the products are of amorphous structure and the density gradually increases with

increasing temperature. The apparent crystalline sizes of β-SiC correspond to the available molecular weight of the original PCs, because the oxygen atoms depress the crystallization.

In the fourth stage, crystal growth of β-SiC occurs accompanied by gas evolution by the reaction between Si-O bonds and the excess carbon. Gas evolution is observed again in the fifth stage.

In the next report, some factors affecting the mechanical properties of SiC fibres will be described.

Acknowledgement

References

1. Y. HASEGAWA and K. OKAMURA, *J. Mater. Sci.* **18** (1983) 3633.
2. *Idem, ibid.* **21** (1986) 321.
3. H. ICHIKAWA, F. MACHIMO, S. MITSUNO, T. ISHIKAWA, K. OKAMURA and Y. HASEGAWA, *ibid.* **21** (1986) 4352.
4. Y. HASEGAWA, M. IIMURA and S. YAJIMA, *ibid.* **15** (1980) 720.
5. W. A. KRINER, *J. Org. Chem.* **29** (1964) 1601.
6. Y. NAGAI, K. YAMAZAKI, N. KOBORI and M. KOSUGI, *Nippon Kagaku Zasshi* **88** (1967) 793.
7. H. SAKURAI, *ibid.* **91** (1970) 885.
8. E. CARBERRY and R. WEST, *J. Organometal. Chem.* **6** (1966) 583.
9. T. MAH, N. L. HECHT, D. E. McCULLUM, J. R. HOENIGMAN, H. M. KIM, A. P. KATZ and H. A. LIPSITT, *J. Mater. Sci.* **19** (1984) 1191.
10. Q. W. PULTZ and W. HERTL, *Trans. Faraday Soc.* **62** (1966) 2499.